

Artificial Cells, Nanomedicine, and Biotechnology

An International Journal

ISSN: 2169-1401 (Print) 2169-141X (Online) Journal homepage: <https://www.tandfonline.com/loi/ianb20>

Green synthesis of zinc oxide nanoparticles using different plant extracts and their antibacterial activity against *Xanthomonas oryzae* pv. *oryzae*

Solabomi Olaitan Ogunyemi, Yasmine Abdallah, Muchen Zhang, Hatem Fouad, Xianxian Hong, Ezzeldin Ibrahim, Md. Mahidul Islam Masum, Afsana Hossain, Jianchu Mo & Bin Li

To cite this article: Solabomi Olaitan Ogunyemi, Yasmine Abdallah, Muchen Zhang, Hatem Fouad, Xianxian Hong, Ezzeldin Ibrahim, Md. Mahidul Islam Masum, Afsana Hossain, Jianchu Mo & Bin Li (2019) Green synthesis of zinc oxide nanoparticles using different plant extracts and their antibacterial activity against *Xanthomonas oryzae* pv. *oryzae*, Artificial Cells, Nanomedicine, and Biotechnology, 47:1, 341-352, DOI: [10.1080/21691401.2018.1557671](https://doi.org/10.1080/21691401.2018.1557671)

To link to this article: <https://doi.org/10.1080/21691401.2018.1557671>



Published online: 29 Jan 2019.



Submit your article to this journal [↗](#)



View Crossmark data [↗](#)

Green synthesis of zinc oxide nanoparticles using different plant extracts and their antibacterial activity against *Xanthomonas oryzae* pv. *oryzae*

Solabomi Olaitan Ogunyemi^{a,b}, Yasmine Abdallah^a, Muchen Zhang^a, Hatem Fouad^{c,d}, Xianxian Hong^a, Ezzeldin Ibrahim^a, Md. Mahidul Islam Masum^a, Afsana Hossain^a, Jianchu Mo^c and Bin Li^a

^aState Key Laboratory of Rice Biology and Ministry of Agriculture Key Lab of Molecular Biology of Crop Pathogens and Insects, Institute of Biotechnology, College of Agricultural and Biotechnology, Zhejiang University, Hangzhou, PR China; ^bDepartment of Crop Protection, Federal University of Agriculture Abeokuta, Abeokuta, Nigeria; ^cMinistry of Agriculture Key Lab of Molecular Biology of Crop Pathogens and Insect Pests, Institute of Insect Sciences, College of Agricultural and Biotechnology, Zhejiang University, Zhejiang, PR China; ^dDepartment of Field Crop Pests, Plant Protection Research Institute, Agricultural Research Center, Cairo, Egypt

ABSTRACT

The synthesis of metal oxide nanoparticles with the use of plant extract is a promising alternative to the conventional chemical method. This work aimed to synthesize zinc oxide nanoparticles (ZnONPs) using plant extract of chamomile flower (*Matricaria chamomilla* L.), olive leaf (*Olea europaea*) and red tomato fruit (*Lycopersicon esculentum* M.). The synthesized ZnONPs were characterized by UV-Visible spectroscopy, Fourier transform infrared spectroscopy (FTIR), X-ray diffraction (XRD), transmission electron microscopy (TEM) and scanning electron microscopy (SEM) with EDS profile. The XRD studies confirmed the presence of pure crystalline shapes of ZnO nanoparticles. The ZnONPs synthesized by *Olea europaea* had the least size range of 40.5 to 124.0 nm as revealed by the SEM observation while XRD revealed a dominant average size of 48.2 nm in the sample which is similar to the size distribution analysis obtained from TEM. The antibacterial effect of ZnONPs synthesized by *Olea europaea* on *Xanthomonas oryzae* pv. *oryzae* (Xoo) strain GZ 0003 had an inhibition zone of 2.2 cm at 16.0 µg/ml which was significantly different from ZnONPs synthesized by *Matricaria chamomilla* and *Lycopersicon esculentum*. Also, the bacterial growth, biofilm formation, swimming motility and bacterial cell membrane of Xoo strain GZ 0003 were significantly affected by ZnO nanoparticle. Overall, zinc oxide nanoparticles are promising biocontrol agents that can be used to combat bacterial leaf blight diseases of rice.

ARTICLE HISTORY

Received 17 September 2018
Revised 27 November 2018
Accepted 29 November 2018

KEYWORDS

Biosynthesis; FTIR; XRD; SEM; plant extracts and antibacterial activity

Introduction





Bacterial leaf blight (BLB) is a worldwide economically important disease of rice crops [1]. The chemical approach has been widely used to combat this diseases, but this leads to environmental pollution and the development of resistant strains. Therefore, the development of biocompatible, bio-safe, and eco-friendly nanomaterials has become a need of the hour for research in the field of nanotechnology.

Recently, metal nanoparticles, carbon nanotubes, and metal oxide nanoparticles having antibacterial effect have been reported [2,3]. Nanoparticles have been used as chemical sensors, anti-corrosive, anti-microbial agents, and in piezoelectric devices [4–6]. Zinc oxide nanoparticles are considered as an elite nanomaterial and grouped with graphene, carbon nanotubes and gold due to their broad applications [7]. It has also been generally recognized as a safe material which is non-toxic, bio-safe and biocompatible [8,9].

Over the years, synthesis of metal nanoparticles has been reported through different methods such as physical,

chemical and biological methods. Biosynthesis of metal nanoparticles using different plants part is a novel option which is without the production of toxic chemicals [10]. Using plant extract to synthesize metal oxide is of significant advantage due to the production of functional molecules which reduce metal ions [11]. The phytochemicals responsible for such synthesis are majorly phenols, terpenoids, ketones, aldehydes and amides [12]. Nanoparticles have been biosynthesized using plant extracts such as *Hibiscus sabdariffa* [13], *Coffea Arabica* [14], *Pueraria tuberosa* [15], *Rheum palmatum* [16], *Nigella arvensis* [17] and *Azadirachta indica* [18].

Among these biosynthesized metal oxide, zinc oxide nanoparticles have been synthesized using leaf extract of aloe barbadensis, *Abutilon indicum*, *Melia azedarach*, *Indigofera tinctoria*, bacterial and fungus [19–22]. Recently, zinc oxide nanoparticles have been green synthesized using: seed extracts of *Nigella sativa* [23], leaf extract of *Psidium guajava* [24], extract of *Daucus carota* [25], plant extract of *Monsonia burkeana* [26], leaf extract of *Mangifera indica* [27], *Aspergillus*

CONTACT Bin Li  libin0571@zju.edu.cn  State Key Laboratory of Rice Biology and Ministry of Agriculture Key Lab of Molecular Biology of Crop Pathogens and Insects, Institute of Biotechnology, College of Agricultural and Biotechnology, Zhejiang University, Hangzhou, PR China; Hatem Fouad Hatem Fouad  dr_hatem@zju.edu.cn  Ministry of Agriculture Key Lab of Molecular Biology of Crop Pathogens and Insect Pests, Institute of Insect Sciences, College of Agricultural and Biotechnology, Zhejiang University, Zhejiang, PR China

© 2019 Informa UK Limited, trading as Taylor & Francis Group

This is an Open Access article distributed under the terms of the Creative Commons Attribution License (<http://creativecommons.org/licenses/by/4.0/>), which permits unrestricted use, distribution, and reproduction in any medium, provided the original work is properly cited.

terreus [28] and *Halomonas elongate* [29]. The antibacterial efficiency of zinc oxide nanoparticles is directly related to its size, shape, surface to volume ratio and number of oxygen vacancy sites [30,31]

Although biosynthesis of zinc oxide has been reported, the potential of plant extracts as biological materials for the synthesis of nanoparticles is yet to be fully explored. Therefore, the aim of this study was the green synthesis of zinc oxide nanoparticles using extracts of chamomile flower (*Matricaria chamomilla* L.), olive leaves (*Olea europaea*), and red tomato fruits (*Lycopersicon esculentum* M.) and evaluation of their antibacterial efficiency against pathogenic bacterial of *Xanthomonas oryzae* pv. *oryzae* strain GZ 0003.

Materials and methods

Preparation of plant extract

Extracts of chamomile flower (*Matricaria chamomilla* L.), olive leaves (*Olea europaea*), and red tomato fruit (*Lycopersicon esculentum* M.) were prepared according to [27,32] with slight modifications. Briefly, chamomile flowers, olive leaves, and red tomato fruits were rinsed in double distilled water and then air-dried. Two grams of finely powdered fruits, flowers, and leaves were extracted in a water bath containing 200 ml of water at 60–70 °C for 4 h. The extracts were then cooled at room temperature and filtered through Whatman filter paper No. 1. The extracts collected were used for the synthesis of zinc oxide nanoparticles.

Preliminary phytochemical testing

Air-dried powdered chamomile flower (*Matricaria chamomilla* L.), olive leaves (*Olea europaea*), and red tomato fruit (*Lycopersicon esculentum* M.) extracts were subjected to preliminary phytochemical testing to detect the presence of the different chemical group of compounds by applying the methods of [33] described elsewhere. The extracts were screened for the presence of terpenes, saponins, alkaloids, flavonoids, tannins, glycosides, and carbohydrates according to the method described by [34,35].

Synthesis of zinc oxide nanoparticles

Zinc oxide was used for the synthesis of zinc oxide nanoparticles according to [36] with slight modification. A ratio of 1:1 of 1 M zinc oxide and the plant extracts were mixed in separate flasks, and the solutions were subjected to continuous heating and stirring at 100 rpm for 4 h. The resultant nanoparticle solution was purified by centrifugation at 10,000 *g* for 20 min. The supernatants were discarded, and the nanoparticles pellet were collected, washed with distilled water, freeze-dried using Alpha 1–2 LDplus and stored at –80 °C.

UV-Vis spectra analysis

The zinc oxide nanoparticles were characterized for its maximum absorbance using UV-Vis spectrophotometry. The

optical property of zinc oxide nanoparticles was analysed by ultraviolet and visible absorption spectroscopy (spectrophotometer Cary E 500) in the range of 200–800 nm.

Transmission electron microscopy (TEM)

The structural characterization and particle size examination of zinc oxide nanoparticles were carried out by Transmission Electron Microscopy (TEM) (JEM-1230, JEOL, Akishima, Japan). The samples were put on the carbon-coated copper grid for 1 min to make a small film of the sample. The excess liquid was removed with a filter paper, and it was then set in a grid box sequentially.

Scanning electron microscopy (SEM)

The structural morphology of zinc oxide nanoparticles was examined and measured by Scanning Electron Microscopic (SEM) using TM-1000, Hitachi, Japan. An aliquot of each sample was fixed on a carbon-coated copper grid, and the film on the SEM grid was then dried by fixing it under a mercury lamp for 5 min. The instrument was equipped with an energy dispersive spectrum (EDS) to ensure the presence of nanoparticles.

Fourier transform infra-red spectroscopy (FT-IR)

The spectra properties of zinc oxide nanoparticles were observed by Fourier transform infrared spectroscopy (FTIR) analysis using the dried powder of the synthesized zinc oxide nanoparticles by FTIR spectrometer vector 22, Bruker, Germany. The pellets were scanned at 4 cm^{–1} resolution in the spectra range of 4000–400 cm^{–1} at room temperature.

X-ray diffraction (XRD)

X-ray diffraction (XRD) studies of the dried nanoparticles were carried out using XPert PRO diffractometer (Holland) with a detector voltage of 40 kV and a current of 30 mA using CuK α radiation. The recorded range of 2 θ was 20–80° with a scanning speed of 6°/min. The estimation of the sizes of particles was performed by Debye–Scherrer's formula.

Determination of minimum inhibitory concentration (MIC)

The minimum inhibitory concentration (MIC) was determined by a broth dilution method assayed in 96-well microtiter plates (Corning-Costar Corp., Corning, NY, USA). The overnight bacterial culture was adjusted to 10⁸ CFU/ml NA Broth. A hundred microliter of bacterial culture was mixed with 100 μ l of two-fold serial dilutions (4.0, 8.0, and 16.0 μ g/ml) of nanoparticles and were subsequently incubated at 30 °C for 48 h. Bacterial culture without nanoparticle served as the control. The minimum inhibitory concentration of nanoparticles was determined by intensity by a Scanning Microplate Spectrophotometer (Thermo Fisher Scientific Inc., Waltham, MA).

Antibacterial activity study

A solution of zinc oxide nanoparticles was tested for antagonism on plate assay previously inoculated with overnight cultured Xoo strain GZ 0003 of 10^8 CFU/ml by dropping 10 μ l of different concentrations of zinc oxide nanoparticles (4.0, 8.0, and 16.0 μ g/ml) in their respective plates and incubated at 30 °C for 18 h. The antibacterial activity was determined by measuring the inhibition zone. The experiment was repeated three times.

Cell viability measurement

The cell viability test was carried out as previously described [37] with slight modifications. Briefly, overnight cultured bacteria of Xoo strain GZ 0003 was diluted to 10^5 CFU/ml which were spread on nutrient agar plate filled with different concentrations of ZnONPs (4.0, 8.0, and 16.0 μ g/ml). A nutrient agar plate not mixed with nanoparticles served as the control. The cells on the plate were counted after incubating at 30 °C for 48 h. The percentage cell viability was calculated using the formula $A_1/A \times 100$, where "A" is the number of colony-forming units on the control plates, "A₁" is the number of the colony-forming unit after using different concentrations of ZnONPs.

Swimming motility assay

The swimming motility assays were tested as previously described [38] with slight modifications. Briefly, a soft agar assay of 0.4% (wt/vol) agar mixed with zinc oxide nanoparticles of 4.0, 8.0, and 16.0 μ g/ml were inoculated with overnight bacterial culture 10^8 CFU/ml, and the plates were incubated at 30 °C for 24 h. A soft agar assay not mixed with nanoparticles served as the control. Swimming motility was evaluated by measuring the migration diameter of the bacterial cells. The motility assay was repeated three times.

Biofilm inhibition assay

Inhibition of bacterial biofilm by zinc oxide nanoparticles was carried out in 96-well plates (Corning-Costar Corp., Corning, NY) by [39] with slight modification. A hundred microliter of Xoo strain GZ 0003 at OD₆₀₀ = 0.8 were added into wells of 96-well plate, and different concentrations of zinc oxide nanoparticles of (4.0, 8.0, and 16.0 μ g/ml) were added while nanoparticle free cell suspension served as the control. The plates were incubated at 30 °C for 48 h. After incubation, the

cultures were discarded, washed thrice with double distilled water to remove unattached cells and air-dried. A hundred microliter of 1% (w/v) aqueous solution of crystal violet was added and kept for 30 min to stain the attached bacterial cells in the wells which were followed by a gentle wash of the wells with double distilled water after discarding the dye in the well. The intensity of the reaction mixture was read spectrophotometrically at 570 nm after the dye was dissolved by the addition of 100 μ l of 33% acetic acid.

Electron microscopy

Bacterial were prepared for electron microscopy as previously described [40] with slight modification. A culture of Xoo strain GZ 0003 was grown to obtain a final concentration of 10^8 CFU/ml. The resulting pellet of 1 ml of bacterial culture was resuspended in 8.0 μ g/ml of zinc oxide nanoparticle after centrifuging at 11,000 *g* for 10 min. The mixture was incubated at 30 °C for 20 min followed by repetitive centrifugation. The cells were washed twice with 0.1 M phosphate buffer (pH 7.2) after they were fixed with 2.5% glutaraldehyde in 0.1 M PBS. Samples were post-fixed with 1% (w/v) Osmium tetroxide (OsO₄) in 0.1 M PBS for 1 h at room temperature, washed once with the same buffer and dehydrated in a graded series of ethanol solutions. The samples were then embedded in Spur low-viscosity embedding medium and thin sections of the specimens were cut with a diamond knife on an Ultracut Ultramicrotome. The sections were double-stained with saturated uranyl acetate and lead citrate. The grids were examined with a JEM-1230 transmission electron microscope (JEOL, Tokyo, Japan) at an operating voltage of 75 kV.

Statistical analysis

The ANOVA test was done using the SAS software (SAS Institute, Cary, USA). Means were compared by the least significant difference (LSD) method at $p < .05$.

Results and discussion

Characterization of zinc oxide nanoparticles

Synthesis of nanoparticles with plant extract is a novel approach which is affordable and eco-friendly [10,41]. The preliminary phytochemical analysis carried out to detect the main constituents of olive leaves, chamomile flower, and tomato fruit is presented in Table 1. The main constituents

Table 1. Phytochemical screening of olive leaves (*Olea europaea*), chamomile flower (*Matricaria chamomilla* L.) and red tomato fruit (*Lycopersicon esculentum* M.) extracts.

Chemical substances	Olive leaves (<i>Olea europaea</i>)	Chamomile flower (<i>Matricaria chamomilla</i> L.)	Red tomato fruit (<i>Lycopersicon esculentum</i> M.)
Terpenes	++	+++	+
Flavonoids	+	+++	++
Saponins	++	—	+
Tannins	++	++	+++
Glycosides / Carbohydrates	++	+	+++
Alkaloids	—	+	+

Present: +; present (high): ++; strongly present: +++; absent: —.

of olive leaves were terpenes, flavonoids, saponins, tannins, and glycosides/carbohydrates while chamomile flower contained majorly, terpenes, flavonoids, tannins, glycosides/carbohydrates, and alkaloids. On the other hand, the tomato fruit extract contained majorly, terpenes, flavonoids, saponins, tannins, glycosides/carbohydrates and alkaloids (Table 1).

In previous studies, use of tomato extract to obtain zinc oxide nanoparticles was effective due to the presence of ascorbic acid which acted as a reducing and capping agent [36] while the flavonoids, glycosides, proteins, and phenols played the vital role of reduction of zinc oxide when olive leaves extract were used [42]. On the other hand, the flavonoids such as flavone, glycosides, and flavonols present in chamomile flower extract acted as the reducing and capping agents for synthesis of zinc oxide [35,43].

The reaction mechanism for the formation of zinc oxide nanoparticles is as a result of the reaction of the zinc ions present in the solution with the polyphenols such as the tannins, glycosides, and flavonoids present in the plant extract forming complexation. This is followed by hydrolysis reaction to form zinc hydroxide due to the presence of the hydroxyl group in the polyphenol. Calcination and decomposition reaction shortly follows to form zinc oxide nanoparticles [44]. Also, the synergistic reaction of all the phytochemical

components present in the extracts (terpenes, flavonoids, saponins, tannins, glycosides/carbohydrates, and alkaloids) act as both reducing and stabilizing agent by reducing Zinc to the 0 valence state [44].

The synthesis of zinc oxide by chamomile flower (*Matricaria chamomilla* L.), olive leaves (*Olea europaea*), and red tomato fruit (*Lycopersicon esculentum* M.) gave an end product of pale white and light brown precipitate respectively (Figure 1). The precipitates were freeze-dried to yield zinc oxide nanopowder which was used for further characterization. The UV – vis spectra of zinc oxide nanoparticles showed a strong absorption band at 384, 380, and 386 nm for chamomile flower (*Matricaria chamomilla* L.), olive leaves (*Olea europaea*), and red tomato fruit (*Lycopersicon esculentum* M.) respectively (Figure 2). The synthesized zinc oxide nanoparticles confirmed in this study by the UV – vis absorption spectra at the wavelength range of 380 to 386 nm which is the characteristic wavelength range of zinc oxide nanoparticles is consistent with the studies of [45]. The synthesized zinc oxide nanoparticles exhibited surface plasmon resonance (SPR) peak at 320 nm which is a blue shift. The band gap energy of SPR was calculated using the formula $E = hc/\lambda$, where “h” is the Plank’s constant, “c” is the velocity of light and “λ” the wavelength. The band gap was found to be 3.88 eV as earlier reported [46].

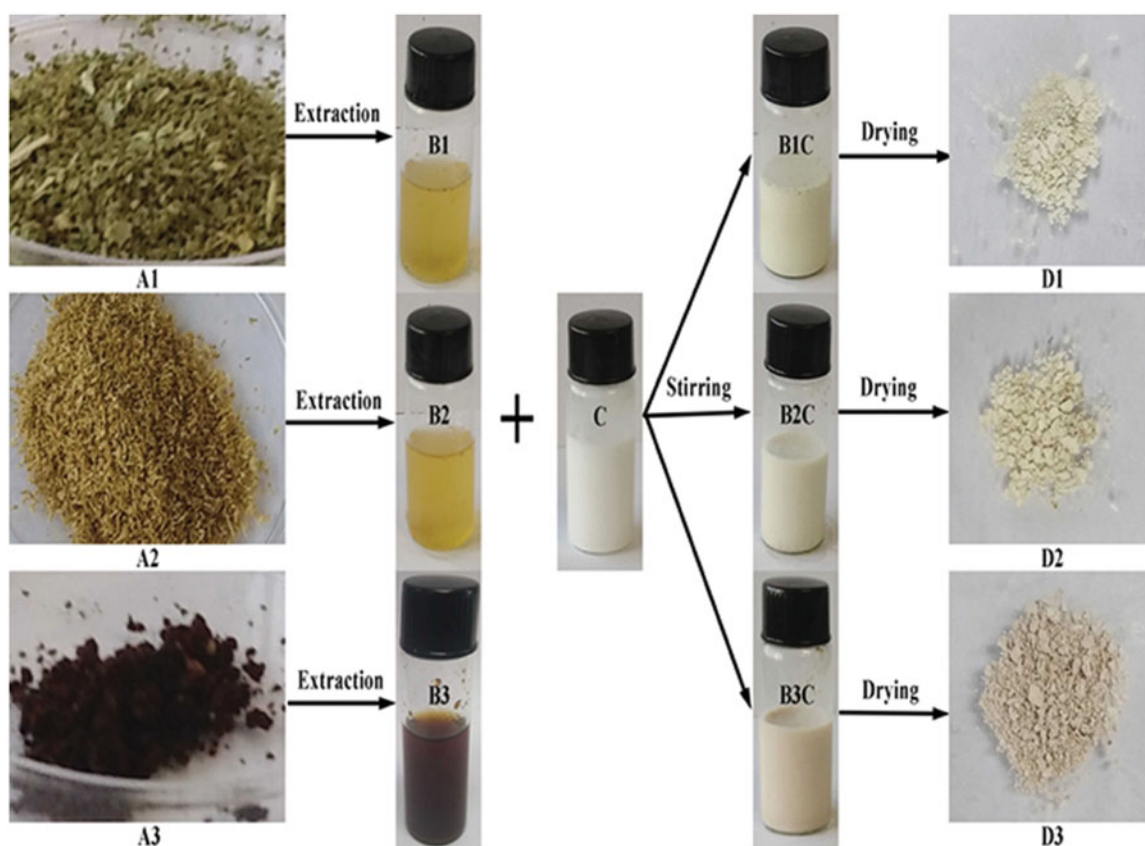


Figure 1. Schematic presentation of zinc oxide nanoparticles synthesis (A1) Olive leaves (*Olea europaea*) (A2) Chamomile flower (*Matricaria chamomilla* L.) (A3) Red tomato fruit (*Lycopersicon esculentum* M.) (B1) Filtered aqueous olive leaves (*Olea europaea*) (B2) Filtered aqueous chamomile flower (*Matricaria chamomilla* L.) (B3) Filtered aqueous red tomato fruit (*Lycopersicon esculentum* M.) (C) Zinc oxide solution (B1C) Synthesized ZnONPs by olive leaves (*Olea europaea*) (B2C) Synthesized ZnONPs by chamomile flower (*Matricaria chamomilla* L.) (B3C) Synthesized ZnONPs by red tomato fruit (*Lycopersicon esculentum* M.) (D1) Dried ZnONPs synthesized by olive leaves (*Olea europaea*) (D2) Dried ZnONPs synthesized by chamomile flower (*Matricaria chamomilla* L.) (D3) Dried ZnONPs synthesized by red tomato fruit (*Lycopersicon esculentum* M.).

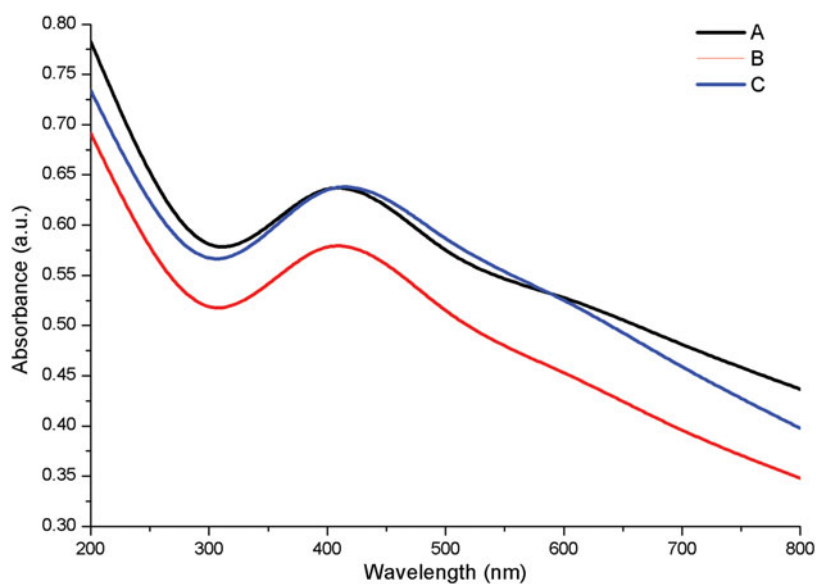


Figure 2. UV-Vis spectra of (A) zinc oxide nanoparticles synthesized by olive leaves (*Olea europaea*) (B) zinc oxide nanoparticles synthesized by chamomile flower (*Matricaria chamomilla* L.) (C) zinc oxide nanoparticles synthesized by red tomato fruit (*Lycopersicon esculentum* M.).

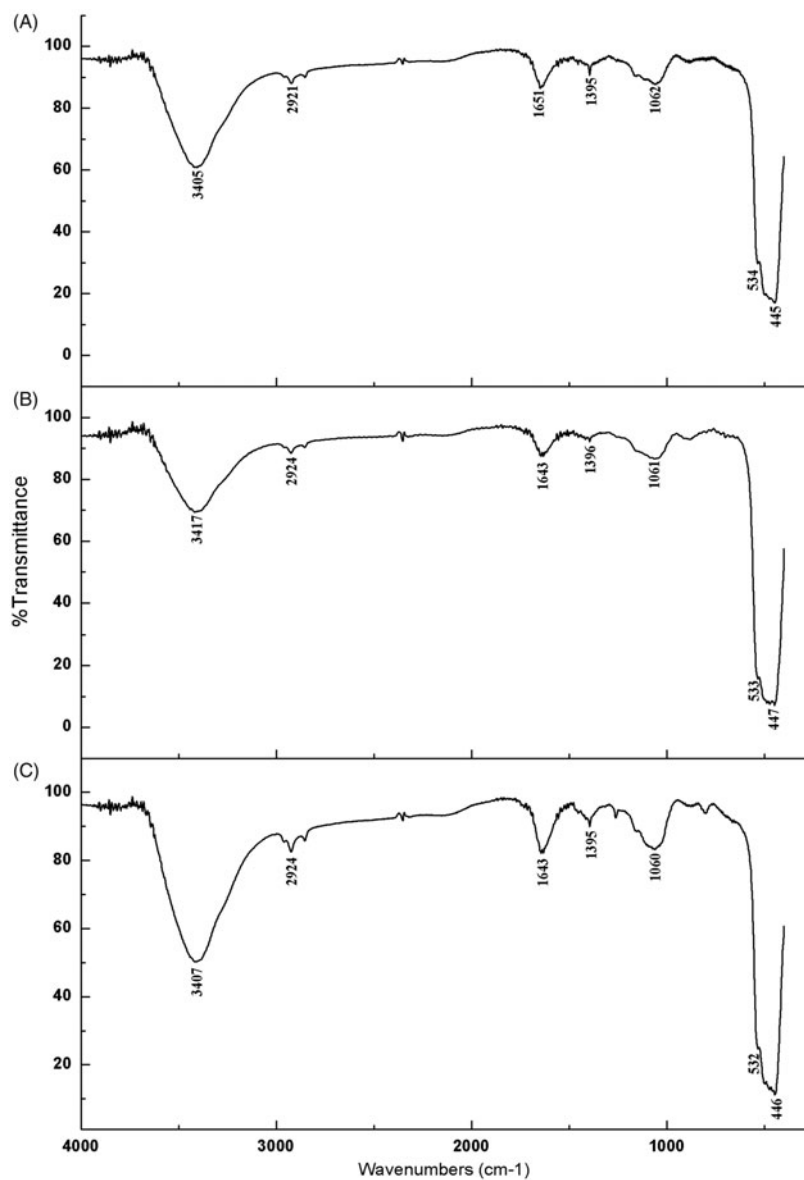


Figure 3. Fourier transform infrared spectra of ZnONPs synthesized by (A) Olive leaves (*Olea europaea*) (B) Chamomile flower (*Matricaria chamomilla* L.) (C) Red tomato fruit (*Lycopersicon esculentum* M.).

The main bands and corresponding assignments common to all the ZnONPs synthesized by chamomile flower (*Matricaria chamomilla* L.), olive leaves (*Olea europaea*), and red tomato fruit (*Lycopersicon esculentum* M.) were as follows: 3407 cm^{-1} , 3417 cm^{-1} , and 3405 cm^{-1} (broad bands of the O-H stretching vibration), 2924 cm^{-1} , and 2921 cm^{-1} (CH_3 stretching vibration), 1643 cm^{-1} , and 1651 cm^{-1} ($\text{C}=\text{O}$ stretching vibration due to the amide 1 group), 1395 cm^{-1} , and 1396 cm^{-1} ($\text{C}-\text{O}-\text{H}$ bending vibration), 1060 cm^{-1} , 1061 cm^{-1} , and 1062 cm^{-1} ($\text{C}-\text{N}$ stretching vibration) while 532 cm^{-1} , 553 cm^{-1} , 534 cm^{-1} , 446 cm^{-1} , 447 cm^{-1} , and 445 cm^{-1} were characteristic bands of the zinc oxide nanoparticles (Figure 3). The FTIR spectrum, absorption at 400 cm^{-1} to 600 cm^{-1} identifies the presence of zinc oxide nanoparticles [47] which further confirms the formation of zinc oxide nanoparticles by using chamomile flower (*Matricaria chamomilla* L.), olive leaves (*Olea europaea*), and red tomato fruit (*Lycopersicon esculentum* M.).

The TEM micrographs show the ZnONPs were cubic structures (Figure 4A) which conformed with the SEM image. Micrographs of TEM indicate that the green synthesized zinc oxide nanoparticles had an average mean size of $41.0 \pm 2.0\text{ nm}$, $51.2 \pm 3.2\text{ nm}$ and $51.6 \pm 3.6\text{ nm}$ for ZnONPs synthesized by *Olea europaea*, *Matricaria chamomilla*, and

Lycopersicon esculentum respectively (Figure 4B). The sizes of the nanoparticles by the SEM ranged from 49.8 nm to 191.0 nm for ZnONPs synthesized by *Matricaria chamomilla*, 40.5 nm to 124.0 nm for ZnONPs synthesized by *Olea europaea*, and a size range of 65.6 nm to 133.0 nm for ZnONPs synthesized by *Lycopersicon esculentum* (Figure 5). The analysis of the samples by energy dispersive spectra (EDS) confirms the elemental structures observed in the samples. The EDS spectrum shows the peak of zinc and oxygen elements to be 81.94 and 18.06% , respectively for ZnONPs synthesized by *Matricaria chamomilla*, 80.84 and 19.16% respectively for ZnONPs synthesized by *Olea europaea*, while 81.97 and 18.03% , respectively, for ZnONPs synthesized by *Lycopersicon esculentum* M. (Figure 6). The EDS analysis obtained shows that the samples prepared using the plant extracts contained pure zinc oxide nanoparticles which are in agreement with [48].

The X-ray diffraction graph showed peaks only due to ZnO (Figure 7). Zinc oxide nanoparticles synthesized by *Olea europaea* showed strong diffraction peaks at 31.7 , 34.4 , 36.3 , 47.6 , 56.6 , 62.9 , 66.4 , 68.0 , 72.6 , 77.0 , 81.1 and 89.6 while ZnONPs synthesized by *Lycopersicon esculentum* had strong diffraction peaks at 31.7 , 34.4 , 36.2 , 47.5 , 56.6 , 62.8 , 66.3 , 67.9 , 75.5 , 76.9 , 81.3 and 89.6 . On the other hand, ZnONPs

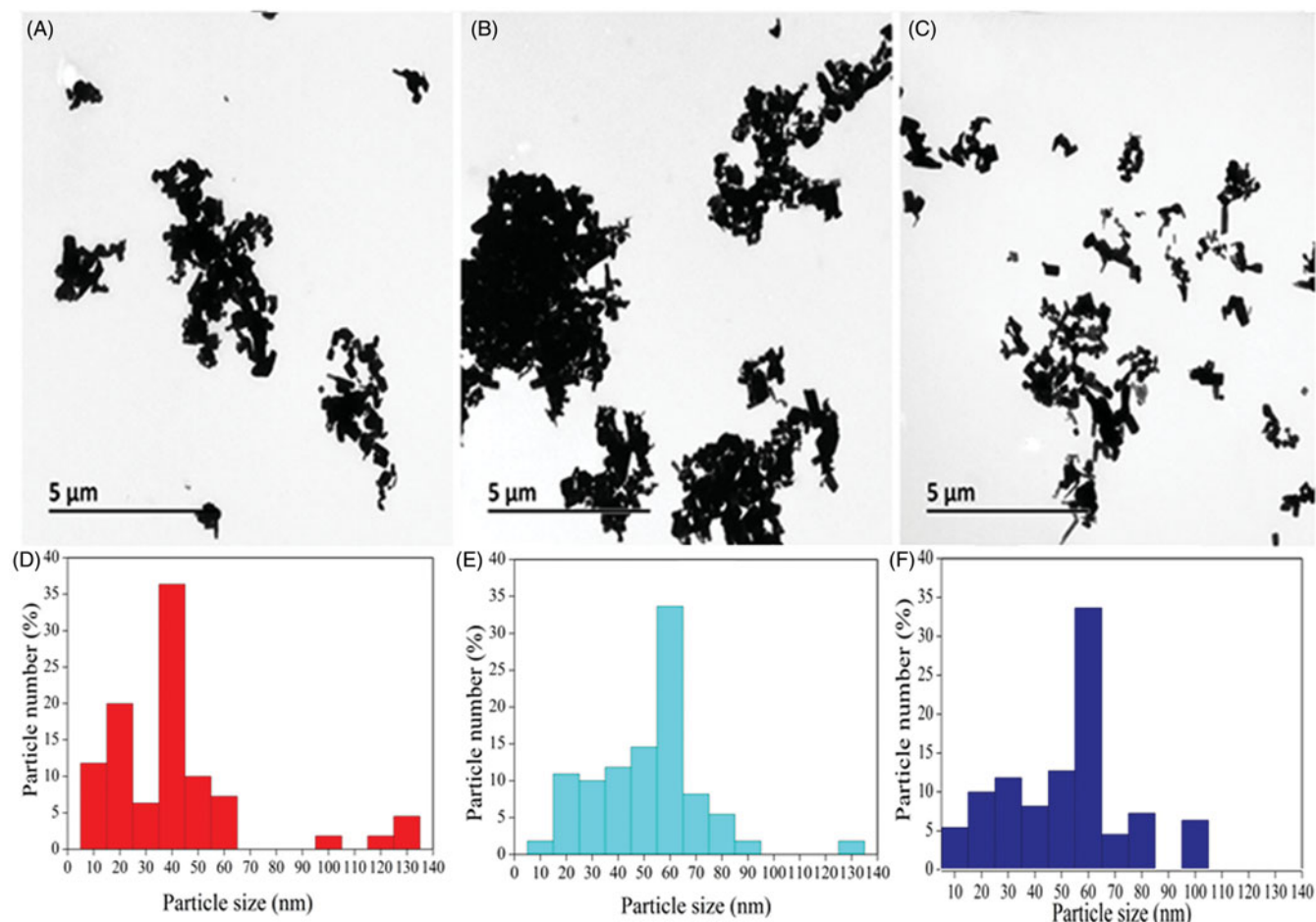


Figure 4. Transmission electron micrographs of synthesized zinc oxide nanoparticles synthesized by (A) Olive leaves (*Olea europaea*) (B) Chamomile flower (*Matricaria chamomilla* L.) (C) Red tomato fruit (*Lycopersicon esculentum* M.). Magnification $5000\times$, Bar = $5\text{ }\mu\text{m}$ and the size distribution of particles in TEM images of zinc oxide nanoparticles synthesized by (D) Olive leaves (*Olea europaea*) (E) Chamomile flower (*Matricaria chamomilla* L.) (F) Red tomato fruit (*Lycopersicon esculentum* M.).

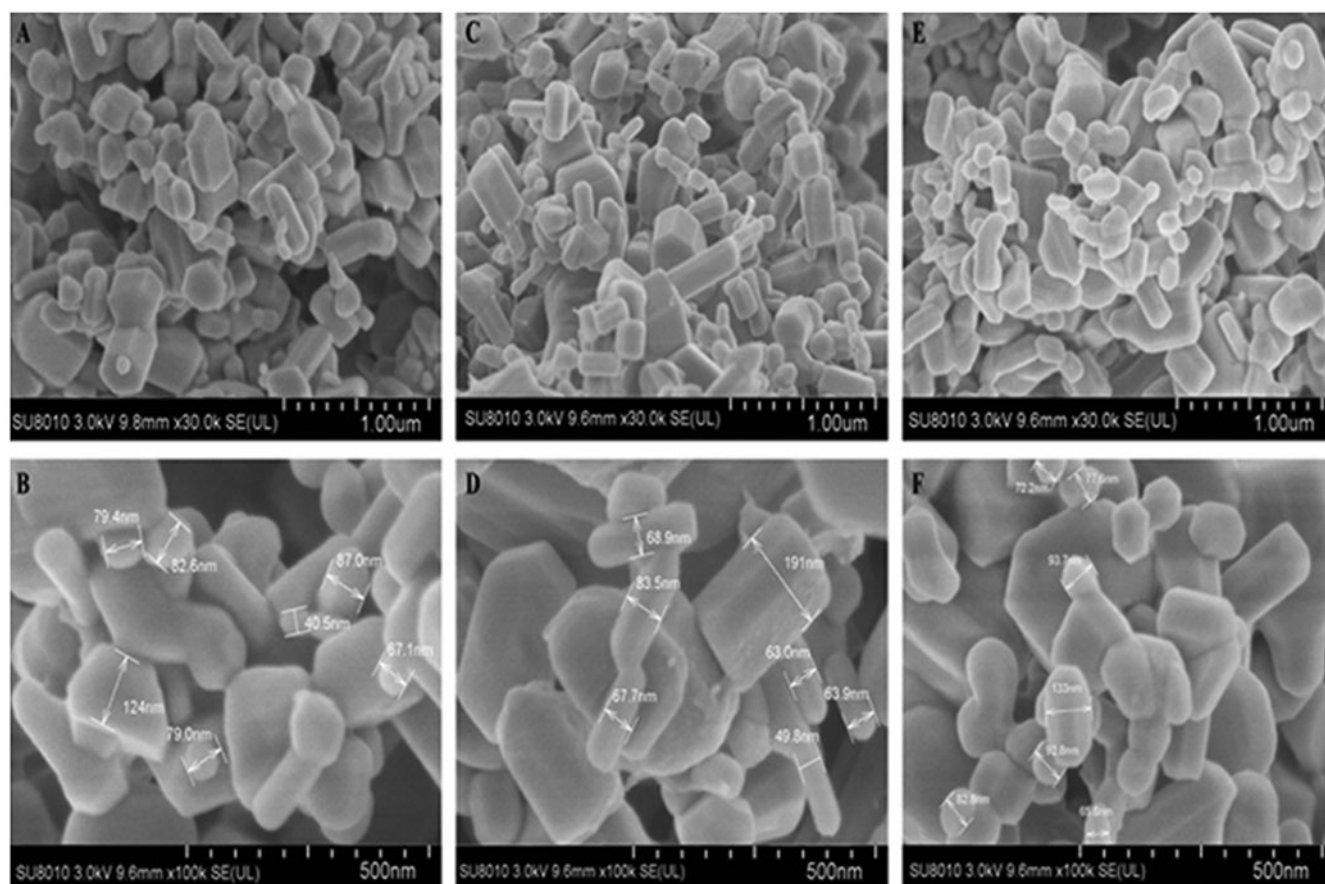


Figure 5. SEM images of the synthesized zinc oxide nanoparticles synthesized using (A, B) Olive leaves (*Olea europaea*) (C, D) Chamomile flower (*Matricaria chamomilla* L.) (E, F) Red tomato fruit (*Lycopersicon esculentum* M.).

synthesized by *Matricaria chamomilla* had strong diffraction peaks at 31.8, 34.5, 36.3, 47.6, 56.6, 62.9, 66.4, 68.0, 72.6, 77.0, 81.4 and 89.7 degrees of 2θ . All the biologically synthesized zinc oxide nanoparticles diffraction peaks corresponded to (100), (002), (101), (102), (110), (103), (200), (112), (004), (202), (104) and (203) crystal planes. The average crystallite sizes of ZnONPs was determined from the width of dominant peaks using the Scherrer equation, and they were 48.2, 65.4 and 61.6 nm respectively, for ZnONPs synthesized by *Olea europaea*, *Matricaria chamomilla*, and *Lycopersicon esculentum*. The Scherrer's equation used to calculate the nanoparticle sizes confirmed smaller particle sizes to be dominant in the synthesized ZnONPs by all the plant extract used which is similar to the size distribution obtained by the TEM. The ZnONPs synthesized by *Olea europaea* contained the smallest dominant particle average sizes of 48.2 nm when compared to those synthesized by *Matricaria chamomilla* and *Lycopersicon esculentum*. The larger nanoparticle sizes observed by the SEM in the samples were due to the agglomeration of smaller nanoparticles.

Antibacterial activity

The antagonist activity of ZnONPs against Xoo strain GZ 0003 was determined by measuring the inhibition zone. The results showed that the inhibitory effect of the ZnONPs increased with increase in the concentration having its

maximum inhibition at 16.0 $\mu\text{g/ml}$ for all the biologically synthesized zinc oxide nanoparticles. Zinc oxide nanoparticles synthesized by *Olea europaea* had the highest inhibition zone of 2.2 cm at 16.0 $\mu\text{g/ml}$ which was significantly different from ZnONPs synthesized by *Matricaria chamomilla* L., and *Lycopersicon esculentum* M. (Figure 8). This result is in concordant with the reports of Fouad and his colleagues who reported the disruption of the growth bacterial by the synthesized silver nanoparticles [49].

The growth of Xoo strain GZ 0003 when different concentrations of ZnONPs were added is shown in Figure 9(A). Strain GZ 0003 had a maximum bacterial number of 1.4 at OD600. At 4.0 $\mu\text{g/ml}$, ZnONPs reduced the bacterial number by 47.5, 38.9, and 34.2% and 59.4, 50.2, and 46.3% at 8.0 $\mu\text{g/ml}$ for zinc oxide synthesized by *Olea europaea*, *Matricaria chamomilla* L., and *Lycopersicon esculentum* M. respectively (Figure 9(A)). Zinc oxide nanoparticles synthesized by *Olea europaea* at 16.0 $\mu\text{g/ml}$ had a 67.5% reduction of the bacterial number at OD600 which was significantly different from the other biologically synthesized zinc oxide (Figure 9(A)).

The minimum inhibitory concentration of ZnONPs on strain GZ 0003 was determined in a 96-well plate using concentrations 4.0, 8.0, and 16.0 $\mu\text{g/ml}$ after 48 h at OD600. The maximum inhibitory concentration was at 16.0 $\mu\text{g/ml}$ for all the biologically synthesized ZnONPs (Figure 9(A)). The results of this study indicated that the growth of Xoo strain GZ 0003 was dependent on the concentrations of nanoparticles, this

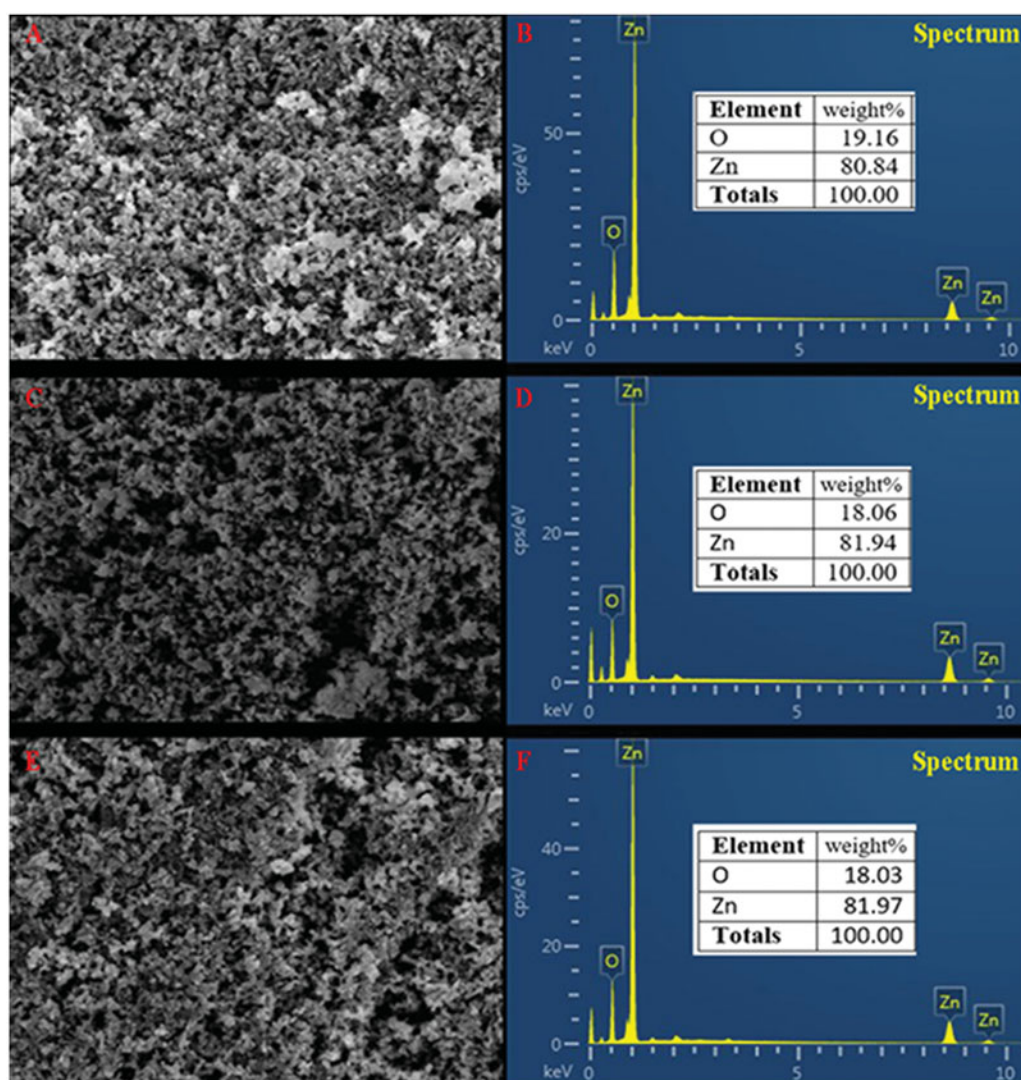


Figure 6. EDS profile of zinc oxide nanoparticles synthesized by (A, B) Olive leaves (*Olea europaea*) (C, D) Chamomile flower (*Matricaria chamomilla* L.) (E, F) Red tomato fruit (*Lycopersicon esculentum* M.).

finding is consistent with the reports of [50] who reported that the higher the concentrations of nanoparticles added, the higher its effect on bacterial growth. Cell viability test was done in order to understand the toxicity level of the nanoparticles against Xoo strain GZ 0003. After incubation with ZnONPs, the formation of the bacterial colonies on the plates was concentration-dependent having the least viable cell at $16.0\mu\text{g/ml}$. The viable cell at $16.0\mu\text{g/ml}$ were 1.02, 1.11, and 2.90% respectively for ZnONPs synthesized by olive leaves, chamomile flower, and red tomato fruit (Figure 9(B)). This result is consistent with previous studies regarding the toxicity of metal oxide nanoparticles against phytopathogens [37,51].

Biofilm formation protects bacterial from external attacks and contributes to bacterial survival during infections [52]. Therefore, the interference with biofilm formation indicates less virulence. In this study, all the synthesized zinc oxide nanoparticles at $16.0\mu\text{g/ml}$ reduced the biofilm formation by 83.3, 79.4, and 75.2% respectively using olive leaves (*Olea europaea*), chamomile flower (*Matricaria chamomilla* L.), and red tomato fruit (*Lycopersicon esculentum* M.) of strain GZ

0003 which had a biofilm formation of 1.5 at OD570 after staining with crystal violet. (Figure 10).

Bacterial swimming motility is directly involved in growth, biofilm formation and pathogenesis [53]. The ability of all the synthesized ZnONPs to significantly reduce the bacterial swimming motility in this study is of significant advantage to the overall management of the bacterial leaf blight diseases. The Xoo strain GZ 0003 swam in the soft LB agar medium and formed halos which reached a diameter of 1.7 cm after 24 h of incubation. Incubation of the soft agar with ZnONPs at $16.0\mu\text{g/ml}$ resulted in a significant decrease in the halo diameter by 48.5, 62.4, and 54.5% for zinc oxide synthesized by *Olea europaea*, *Matricaria chamomilla* L., and *Lycopersicon esculentum* M. respectively. All the biologically synthesized ZnONPs were not significantly different from each other in the reduction of the halo diameter (Figure 11). The ability of the nanoparticles to reduce biofilm formation and swimming motility of the bacterial is consistent with the studies of [54].

Examination of the antibacterial activity of all the biologically synthesized ZnONPs on Xoo strain GZ 0003 was observed under transmission electron microscopy. It was observed that

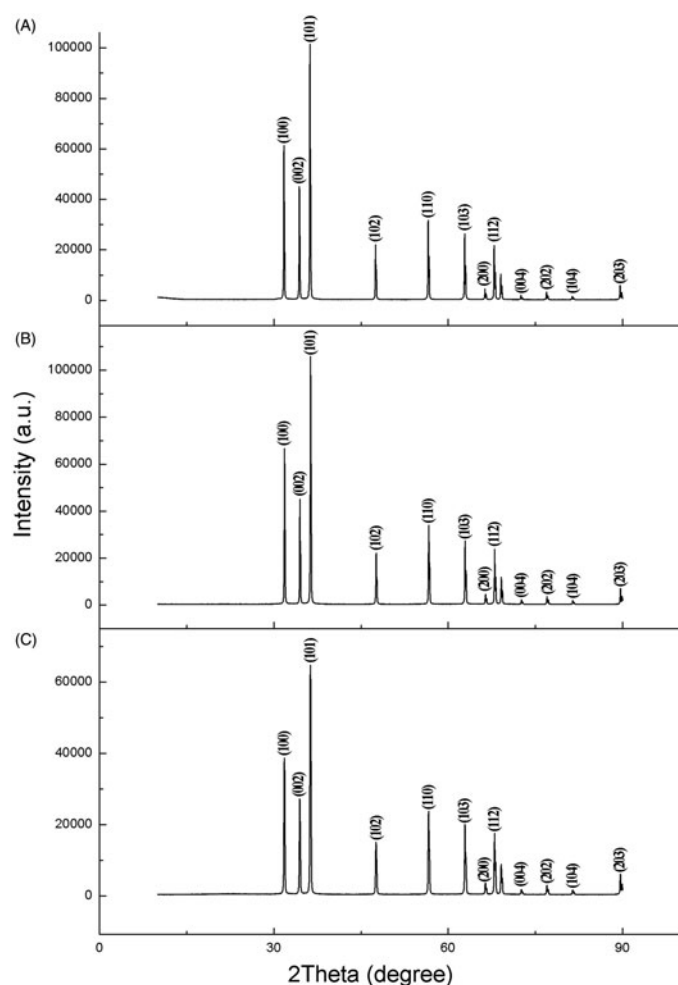


Figure 7. XRD spectra of synthesized zinc oxide nanoparticles using (A) Olive leaves (*Olea europaea*) (B) Chamomile flower (*Matricaria chamomilla* L.) (C) Red tomato fruit (*Lycopersicon esculentum* M.).

the control without nanoparticles treatment had intact cell membrane with abundant bacterial cytoplasm while GZ 0003 treated with all the biologically synthesized nanoparticles revealed collapsed and ruptured cell membrane with leakage of the bacterial cytoplasm (Figure 12). The inhibition zones caused by all the ZnONPs on Xoo strain GZ 0003 growth could be as a result of the damaged bacterial cell membrane and leakage of cytoplasm as observed under the transmission electron microscopy, therefore, leading to the death of the bacterium. This result is in agreement with the reports of [16,55] who reported an inhibition zone caused by ZnONPs against *Pseudomonas aeruginosa* and *Enterobacter aerogens*.

The mechanism of antibacterial activity of ZnONPs is mainly by interacting with the bacterial membrane which leads to collapse and rupture of the membrane and this results in the leakage of bacterial cytoplasm [3]. The antibacterial properties of ZnONPs can be attributed to the oxidative stress induced by Reactive Oxygen Species (ROS) generation from its surface which causes the tear down of bacterial membrane. ROS composed of molecules, such as oxygen, $\text{HO}_2\cdot$ (per hydroxyl radicals), $\text{O}_2^{\cdot-}$ (superoxide anion), and the hydroxyl radical (OH), which can damage DNA, RNA and

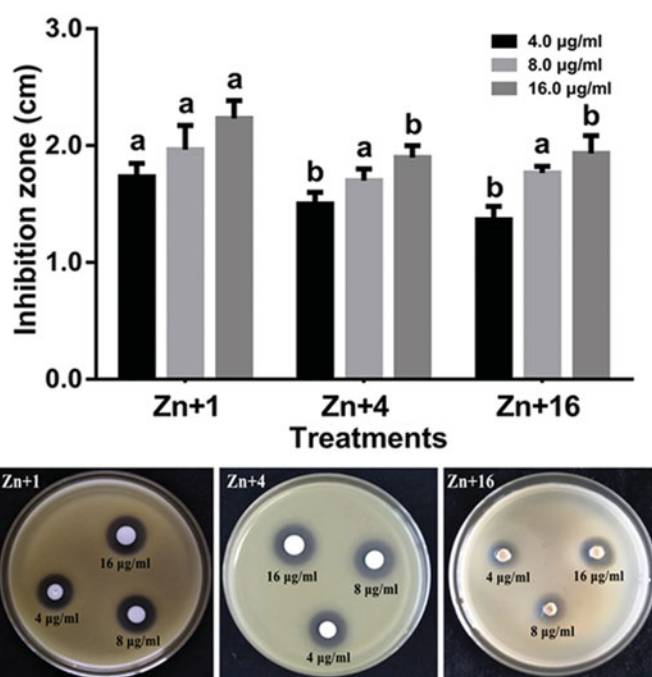


Figure 8. Antibacterial activity of zinc oxide nanoparticles against strain GZ 0003 of *Xanthomonas oryzae* pv. *oryzae*. Plates are showing inhibition zones on strain GZ 0003 of *Xanthomonas oryzae* pv. *oryzae* caused by zinc oxide nanoparticles *Zn + 1 zinc oxide nanoparticles synthesized by olive leaves (*Olea europaea*) Zn + 4 zinc oxide nanoparticles synthesized by chamomile flower (*Matricaria chamomilla* L.) Zn + 16 zinc oxide nanoparticles synthesized by red tomato fruit (*Lycopersicon esculentum* M.). *Values are a mean \pm standard error of three replicates and bars with the same letters are not significantly different in LSD test ($p < .05$).

oxidize proteins and lipids, thereby leading to bacterial decomposition and death [56].

Previous studies reported a variation in the degree of the intensity of ROS Gram-negative and Gram-positive bacteria treated with ZnONPs when observed under a fluorescence spectrophotometer with (dichlorofluorescein diacetate) DCFH-DA. DCFH-DA is a nonpolar dye which is converted into its polar derivative DCFH by cellular esterase; DCFH is not fluorescent but converts into the highly fluorescent DCF when oxidized by ROS. The higher fluorescence intensity observed indicates that more DCFH transform to DCF by the oxidation of ROS due to treatment with ZnONPs [3]. Also, the antibacterial mechanism of ZnONPs is attributed to the release of Zn^{2+} out of the cell when they reach toxic concentration which strongly binds to the thiol group of proteins and enzymes on the cellular surface, thereby causing bacterial death [3,57].

Conclusion

In this study, zinc oxide nanoparticles were successfully bio-synthesized using plant extracts of olive leaves (*Olea europaea*), chamomile flower (*Matricaria chamomilla* L.), and red tomato fruit (*Lycopersicon esculentum* M.). The resultant nanoparticles were characterized using UV – Visible spectroscopy, FTIR, XRD, SEM, TEM, and EDS. The antibacterial activity of the ZnONPs were examined on Xoo strain GZ 0003 and it was discovered that zinc oxide synthesized by olive leaves (*Olea europaea*) at $16.0 \mu\text{g mL}^{-1}$ had the highest significant

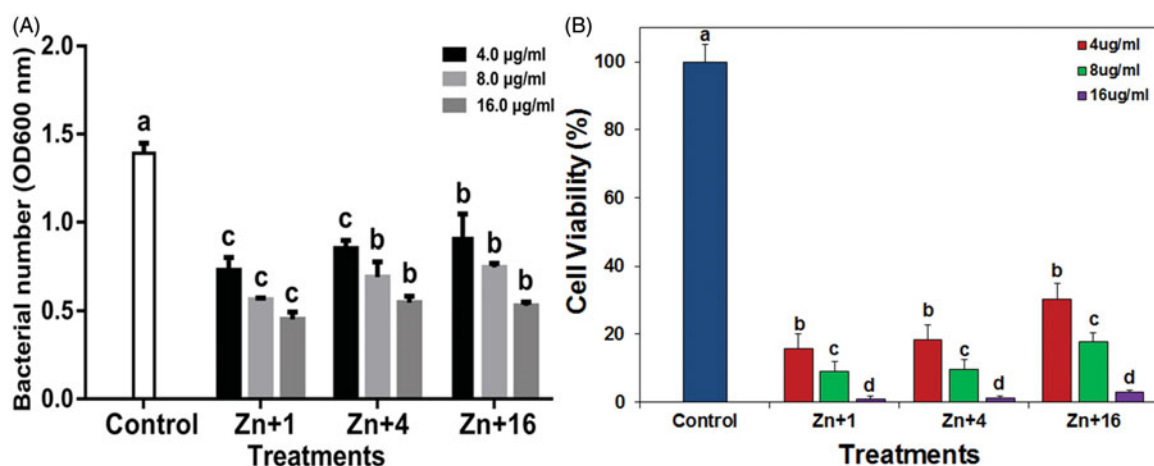


Figure 9. (A) Effect of zinc oxide nanoparticles on the growth of strain GZ 0003 of *Xanthomonas oryzae* pv. *oryzae*. (B) Percentage viable cell of strain GZ 0003 of *Xanthomonas oryzae* pv. *oryzae* after treatment with zinc oxide nanoparticles *Zn + 1 zinc oxide nanoparticles synthesized by olive leaves (*Olea europaea*) Zn + 4 zinc oxide nanoparticles synthesized by chamomile flower (*Matricaria chamomilla* L.) Zn + 16 zinc oxide nanoparticles synthesized by red tomato fruit (*Lycopersicon esculentum* M.). *Values are a mean \pm standard error of three replicates and bars with the same letters are not significantly different in LSD test ($p < .05$).

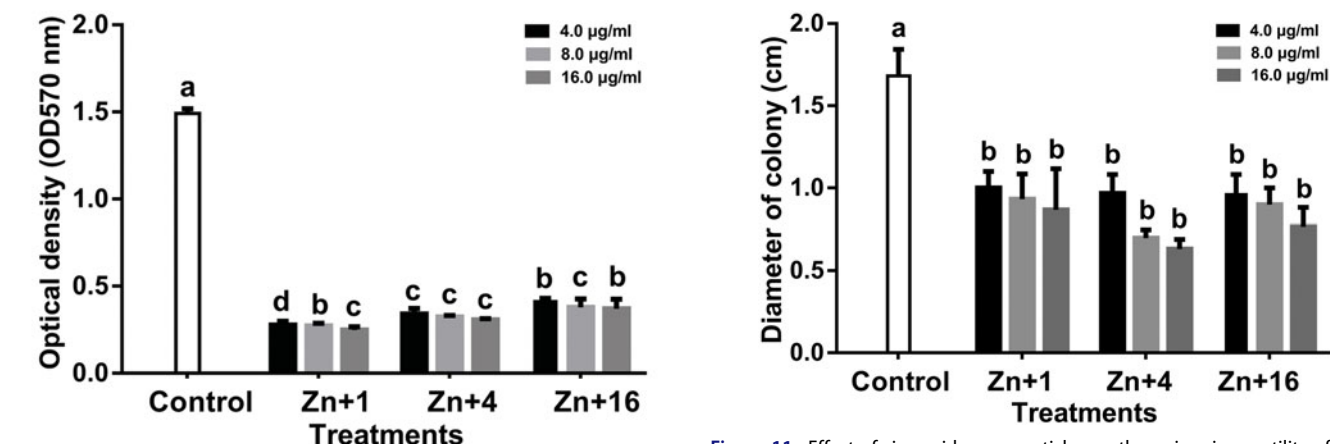


Figure 11. Effect of zinc oxide nanoparticles on the swimming motility of strain GZ 0003 of *Xanthomonas oryzae* pv. *oryzae*. *Zn + 1 zinc oxide nanoparticles synthesized by olive leaves (*Olea europaea*) Zn + 4 zinc oxide nanoparticles synthesized by chamomile flower (*Matricaria chamomilla* L.) Zn + 16 zinc oxide nanoparticles synthesized by red tomato fruit (*Lycopersicon esculentum* M.). *Values are a mean \pm standard error of three replicates and bars with the same letters are not significantly different in LSD test ($p < .05$).

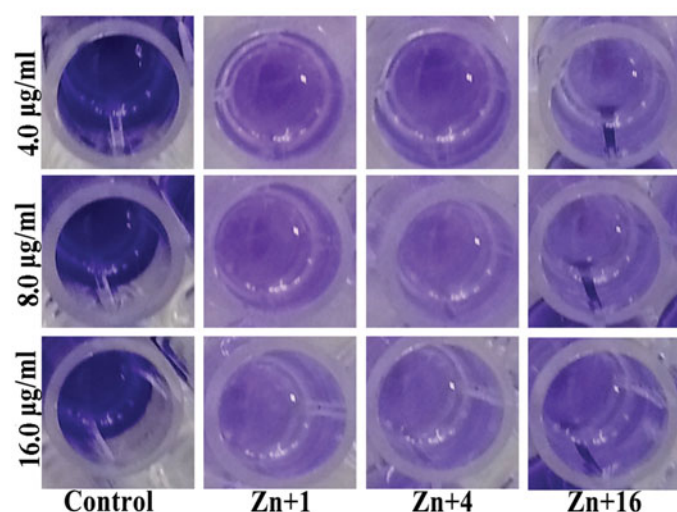


Figure 10. Effect of synthesized zinc oxide nanoparticles on biofilm formation of strain GZ 0003 of *Xanthomonas oryzae* pv. *oryzae*. *Zn + 1 zinc oxide nanoparticles synthesized by olive leaves (*Olea europaea*) Zn + 4 zinc oxide nanoparticles synthesized by chamomile flower (*Matricaria chamomilla* L.) Zn + 16 zinc oxide nanoparticles synthesized by red tomato fruit (*Lycopersicon esculentum* M.). *Values are a mean \pm standard error of three replicates and bars with the same letters are not significantly different in LSD test ($p < .05$).

antibacterial activity in the bacterial inhibition zone, bacterial growth and biofilm formation which could be attributed to

its dominant crystallite small size of 48.2 nm as compared to others. Our findings reveal that the size of the synthesized ZnONPs was essential for their efficient antibacterial activity. Overall, the synthesized zinc oxide nanoparticles were found to be an effective antimicrobial agent against the causal organism of bacterial leaf blight.

Disclosure statement

The authors declare that the research was conducted in the absence of any commercial or financial relationships that could be construed as a potential conflict of interest.

Funding

This work was supported by Zhejiang Provincial Natural Science Foundation of China (LZ19C140002), National Natural Science Foundation of China (31872017, 31571971, 31371904, 31801787), Zhejiang Provincial Project (2017C02002, 2018C02G2071267), National Key Research and Development Program of China (2017YFD0201104),

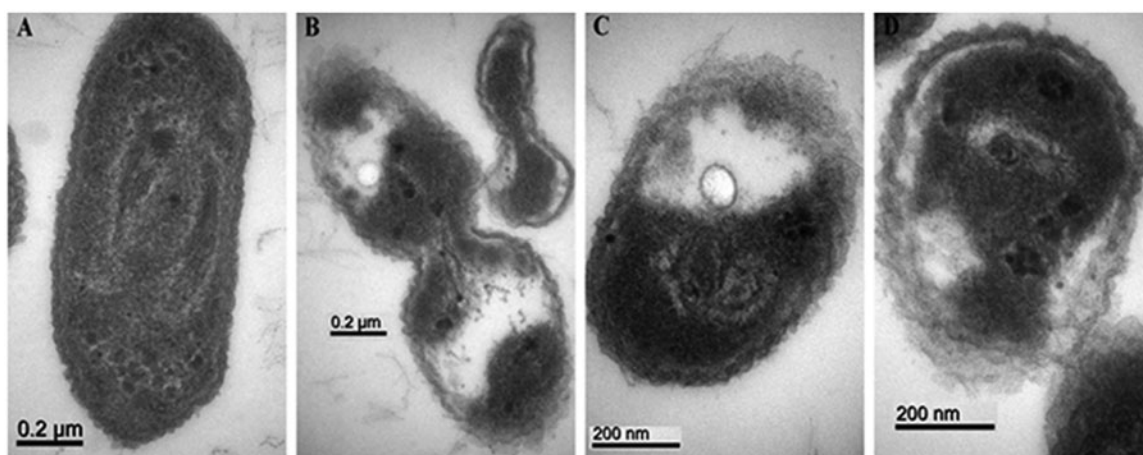


Figure 12. TEM images of strain GZ 0003 of *Xanthomonas oryzae* pv. *oryzae* (A) treated with double distilled water, and treatment with 8 µg/ml of zinc oxide nanoparticles synthesized by (B) Olive leaves (*Olea europaea*) (C) Chamomile flower (*Matricaria chamomilla* L.), (D) Red tomato fruit (*Lycopersicon esculentum* M). Magnification 100,000× for A and B; 150,000× for C and D; Bar = 0.2 µm for A and B; 200 nm for C and D.

Shanghai Agricultural Basic Research Project (2014:7-3-1), Key Scientific Technological Project of Ningbo (2016C11017), the Fundamental Research Funds for the Central Universities, Dabeinong Funds for Discipline Development and Talent Training in Zhejiang University, Key Subject Construction Program of Zhejiang for Modern Agricultural Biotechnology and Crop Disease Control.

References

- [1] Mew TW. Current status and future-prospects of research on bacterial-blight of rice. *Annu Rev Phytopathol.* 1987;25: 359–382.
- [2] Prasanna VL, Vijayaraghavan R. Insight into the mechanism of antibacterial activity of ZnO: surface defects mediated reactive oxygen species even in the dark. *Langmuir.* 2015;31:9155–9162.
- [3] Zhong L, Liu H, Samal M, et al. Synthesis of ZnO nanoparticles-decorated spindle-shaped graphene oxide for application in synergistic antibacterial activity. *J Photochem Photobiol B-Biol.* 2018; 183:293–301.
- [4] Fujihara S, Naito H, Kimura T. Visible photoluminescence of ZnO nanoparticles dispersed in highly transparent MgF₂ thin-films via sol-gel process. *Thin Solid Films.* 2001;389:227–232.
- [5] Mochinaga R, Yamasaki T, Arakawa T. The gas-sensing of SmCoO_x/MO_x (M=Fe, Zn, In, Sn) having a heterojunction. *Sens Actuators B-Chem.* 1998;52:96–99.
- [6] Siyanbola TO, Sasidhar K, Anjaneyulu B, et al. Anti-microbial and anti-corrosive poly (ester amide urethane) siloxane modified ZnO hybrid coatings from Thevetia peruviana seed oil. *J Mater Sci.* 2013;48:8215–8227.
- [7] Kumar S, Ahlawat W, Kumar R, et al. Graphene, carbon nanotubes, zinc oxide and gold as elite nanomaterials for fabrication of biosensors for healthcare. *Biosens Bioelectron.* 2015;70:498–503.
- [8] Raghupathi KR, Koodali RT, Manna AC. Size-dependent bacterial growth inhibition and mechanism of antibacterial activity of zinc oxide nanoparticles. *Langmuir.* 2011;27:4020–4028.
- [9] Rosi NL, Mirkin CA. Nanostructures in biodiagnostics. *Chem Rev.* 2005;105:1547–1562.
- [10] Okitsu K, Mizukoshi Y, Yamamoto TA, et al. Sonochemical synthesis of gold nanoparticles on chitosan. *Mater Lett.* 2007;61: 3429–3431.
- [11] Rai M, Ingle A. Role of nanotechnology in agriculture with special reference to management of insect pests. *Appl Microbiol Biotechnol.* 2012;94:287–293.
- [12] Sundrarajan M, Gowri S. Green synthesis of titanium dioxide nanoparticles by nycanthes arbor-tristis leaves extract. *Chalcogenide Lett.* 2011;8:447–451.
- [13] Thovhogi N, Diallo A, Gurib-Fakim A, et al. Nanoparticles green synthesis by *Hibiscus sabdariffa* flower extract: main physical properties. *J Alloys Compounds.* 2015;647:392–396.
- [14] Dhand V, Soumya L, Bharadwaj S, et al. Green synthesis of silver nanoparticles using *Coffea arabica* seed extract and its antibacterial activity. *Mater Sci Eng C-Mater Biol Appl.* 2016;58:36–43.
- [15] Satpathy S, Patra A, Ahirwar B, et al. Antioxidant and anticancer activities of green synthesized silver nanoparticles using aqueous extract of tubers of *Pueraria tuberosa*. *Artif Cells Nanomed Biotechnol.* 2018;1–15. doi: 10.1080/21691401.2018.1489265.
- [16] Arokiyaraj S, Vincent S, Saravanan M, et al. Green synthesis of silver nanoparticles using *Rheum palmatum* root extract and their antibacterial activity against *Staphylococcus aureus* and *Pseudomonas aeruginosa*. *Artif Cells Nanomed Biotechnol.* 2017; 45:372–379.
- [17] Chahardoli A, Karimi N, Sadeghi F, et al. Green approach for synthesis of gold nanoparticles from *Nigella arvensis* leaf extract and evaluation of their antibacterial, antioxidant, cytotoxicity and catalytic activities. *Artif Cells Nanomed Biotechnol.* 2018;46:579–588.
- [18] Velusamy P, Das J, Pachaiappan R, et al. Greener approach for synthesis of antibacterial silver nanoparticles using aqueous solution of neem gum (*Azadirachta indica* L.). *Ind Crop Prod.* 2015;66: 103–109.
- [19] Jain N, Bhargava A, Tarafdar JC, et al. A biomimetic approach towards synthesis of zinc oxide nanoparticles. *Appl Microbiol Biotechnol.* 2013;97:859–869.
- [20] Jayaseelan C, Rahuman AA, Kirthi AV, et al. Novel microbial route to synthesize ZnO nanoparticles using *Aeromonas hydrophila* and their activity against pathogenic bacteria and fungi. *Spectrochim Acta A Mol Biomol Spectrosc.* 2012;90:78–84.
- [21] Prashanth GK, Prashanth PA, Nagabhushana BM, et al. Comparison of anticancer activity of biocompatible ZnO nanoparticles prepared by solution combustion synthesis using aqueous leaf extracts of *Abutilon indicum*, *Melia azedarach* and *Indigofera tinctoria* as biofuels. *Artif Cells Nanomed Biotechnol.* 2018;46: 968–979.
- [22] Sangeetha G, Rajeshwari S, Venckatesh R. Green synthesis of zinc oxide nanoparticles by aloe barbadensis miller leaf extract: structure and optical properties. *Mater Res Bull.* 2011;46:2560–2566.
- [23] Alaghemand A, Khaghani S, Bihanta MR, et al. Green synthesis of zinc oxide nanoparticles using *Nigella sativa* L. extract: the effect on the height and number of branches. *J Nanostruct.* 2018;8: 82–88.
- [24] Saha R, Karthik S, Kumar PMRSA, et al. *Psidium guajava* leaf extract-mediated synthesis of ZnO nanoparticles under different processing parameters for hydrophobic and antibacterial finishing over cotton fabrics. *Prog Org Coat.* 2018;124:80–91.

- [25] Luque PA, Nava O, Soto-Robles CA, et al. Effects of *Daucus carota* extract used in green synthesis of zinc oxide nanoparticles. *J Mater Sci: Mater Electron*. 2018;29:17638–17643. doi:10.1007/s10854-018-9867-5.
- [26] Ngoepe NM, Mbita Z, Mathipa M, et al. Biogenic synthesis of ZnO nanoparticles using *Monsonia burkeana* for use in photocatalytic, antibacterial and anticancer applications. *Ceram Int*. 2018;44:16999–17006.
- [27] Rajeshkumar S, Kumar SV, Ramaiah A, et al. Biosynthesis of zinc oxide nanoparticles using *Mangifera indica* leaves and evaluation of their antioxidant and cytotoxic properties in lung cancer (A549). *Enzyme Microb Technol*. 2018;117:91–95.
- [28] Fouda A, Hassan SED, Salem SS, et al. *In-vitro* cytotoxicity, antibacterial and UV-protection properties of the biosynthesized zinc oxide nanoparticles for medical textile applications. *Microbial Pathogenesis*. 2018;125:252–261.
- [29] Taran M, Rad M, Alavi M. Biosynthesis of TiO₂ and ZnO nanoparticles by *Halomonas elongata* IBRC-M 10214 in different conditions of media. *Bl*. 2017;8:81–89.
- [30] Fu FY, Li LY, Liu LJ, et al. Construction of cellulose based ZnO nanocomposite films with antibacterial properties through one-step coagulation. *Acs Appl Mater Interfaces*. 2015;7:2597–2606.
- [31] Guo HY, He XM, Hu CG, et al. Effect of particle size in aggregates of ZnO-aggregate-based dye-sensitized solar cells. *Electrochim Acta*. 2014;120:23–29.
- [32] Prakash MB, Paul S. Green synthesis of silver nanoparticles using vinca roseus leaf extract and evaluation of their antimicrobial activities. *Int J Appl Biol Pharma Technol*. 2012;3:105–111.
- [33] Tona L, Kambu K, Ngimbi N, et al. Antiamoebic and phytochemical screening of some Congolese medicinal plants. *J Ethnopharmacol*. 1998;61:57–65.
- [34] Arokiyaraj S, Dinesh Kumar V, Elakya V, et al. Biosynthesized silver nanoparticles using floral extract of *Chrysanthemum indicum* L.–potential for malaria vector control. *Environ Sci Pollut Res*. 2015;22:9759–9765.
- [35] Fouad H, Hongjie L, Hosni D, et al. Controlling *Aedes albopictus* and *Culex pipiens* pallens using silver nanoparticles synthesized from aqueous extract of Cassia fistula fruit pulp and its mode of action. *Artif Cell Nanomed Biotechnol*. 2018;46:558–567.
- [36] Sutradhar P, Saha A. Green synthesis of zinc oxide nanoparticles using tomato (*Lycopersicon esculentum*) extract and its photovoltaic application. *J Exp Nanosci*. 2016;11:314–327.
- [37] Cai L, Chen J, Liu Z, et al. Magnesium oxide nanoparticles: effective agricultural antibacterial agent against *Ralstonia solanacearum*. *Front Microbiol*. 2018;9:790.
- [38] Rashid MH, Kornberg A. Inorganic polyphosphate is needed for swimming, swarming, and twitching motilities of *Pseudomonas aeruginosa*. *Proc Natl Acad Sci USA*. 2000;97:4885–4890.
- [39] Hassan A, Usman J, Kaleem F, et al. Evaluation of different detection methods of biofilm formation in the clinical isolates. *Brazilian J Infect Dis*. 2011;15:305–311.
- [40] Helander IM, Nurmiaho-Lassila EL, Ahvenainen R, et al. Chitosan disrupts the barrier properties of the outer membrane of Gram-negative bacteria. *Int J Food Microbiol*. 2001;71:235–244.
- [41] Barman G, Maiti S, Laha JK. Bio-fabrication of gold nanoparticles using aqueous extract of red tomato and its use as a colorimetric sensor. *Nanoscale Res Lett*. 2013;8:181–190. doi:10.1186/1556-276x-8-181.
- [42] Hashemi S, Asrar Z, Pourseyedi S, et al. Green synthesis of ZnO nanoparticles by Olive (*Olea europaea*). *Int Nanobiotechnol*. 2016;10:400–404.
- [43] Harbourne N, Jacquier JC, O'Riordan D. Optimisation of the extraction and processing conditions of chamomile (*Matricaria chamomilla* L.) for incorporation into a beverage. *Food Chem*. 2009;115:15–19.
- [44] Basnet P, Chanu TI, Samanta D, et al. A review on bio-synthesized zinc oxide nanoparticles using plant extracts as reductants and stabilising agents. *J Photochem Photobiol B Biol*. 2018;183:201–221.
- [45] Mohammadian M, Es'haghi Z, Hooshmand S. Green and chemical synthesis of zinc oxide nanoparticles and size evaluation by UV – vis spectroscopy. *J Nanomed Res*. 2018;1:7.
- [46] Bhuyan T, Mishra K, Khanuja M, et al. Biosynthesis of zinc oxide nanoparticles from *Azadirachta indica* for antibacterial and photocatalytic applications. *Mater Sci Semicond Process*. 2015;32:55–61.
- [47] Yuvakkumar R, Suresh J, Saravanakumar B, et al. Rambutan peels promoted biomimetic synthesis of bioinspired zinc oxide nano-chains for biomedical applications. *Spectrochim Acta A Mol Biomol Spectrosc*. 2015;137:250–258.
- [48] Kumar SS, Venkateswarlu P, Rao Rao VR, et al. Synthesis, characterization and optical properties of zinc oxide nanoparticles. *International Nano Lett*. 2013;3:30–36. doi:10.1186/2228-5326-3-30.
- [49] Fouad H, Hongjie L, Yanmei D, et al. Synthesis and characterization of silver nanoparticles using *Bacillus amyloliquefaciens* and *Bacillus subtilis* to control filaria vector *Culex pipiens* pallens and its antimicrobial activity. *Artif Cells Nanomed Biotechnol*. 2017;45:1369–1378.
- [50] Duffy LL, Osmond-McLeod MJ, Judy J, et al. Investigation into the antibacterial activity of silver, zinc oxide and copper oxide nanoparticles against poultry-relevant isolates of *Salmonella* and *Campylobacter*. *Food Control*. 2018;92:293–300.
- [51] Dizaj SM, Lotfipour F, Barzegar-Jalali M, et al. Antimicrobial activity of the metals and metal oxide nanoparticles. *Mater Sci Eng C-Mater Biol Appl*. 2014;44:278–284.
- [52] Bridier A, Briandet R, Thomas V, et al. Resistance of bacterial biofilms to disinfectants: a review. *Biofouling*. 2011;27:1017–1032.
- [53] Ahmad AA, Askora A, Kawasaki T, et al. The filamentous phage XacF1 causes loss of virulence in *Xanthomonas axonopodis* pv. citri, the causative agent of citrus canker disease. *Front Microbiol*. 2014;5:1–11. doi:10.3389/fmicb.2014.00321.
- [54] Alavi M, Karimi N. Antiplanktonic, antibiofilm, anti-swarming motility and anti-quorum sensing activities of green synthesized Ag-TiO₂, TiO₂-Ag, Ag-Cu and Cu-Ag nanocomposites against multi-drug-resistant bacteria. *Artif Cell Nanomed Biotechnol*. 2018;1:1–5. doi:10.1080/21691401.2018.146923.
- [55] Rajabairavi N, Raju CS, Karthikeyan C, et al. Biosynthesis of novel zinc oxide nanoparticles (ZnO NPs) using endophytic bacteria *Sphingobacterium thalpophilum*. In Ebenezer J, editor. *Recent Trends Mater Sci Appl*. 2017;189:245–254.
- [56] Krishnamoorthy K, Veerapandian M, Zhang L-H, et al. Antibacterial efficiency of graphene nanosheets against pathogenic bacteria via lipid peroxidation. *J Phys Chem C*. 2012;116:17280–17287.
- [57] Agarwal H, Menon S, Venkat-Kumar S, et al. Mechanistic study of the antibacterial action of zinc oxide nanoparticles synthesized using green route. *Chemico-Biol Inter*. 2018;286:60–70.